



AN ALGAN/GAN BASED UV PHOTODETECTOR SIMULATION USING COMSOL TO OBTAIN THE FRESNEL COEFFICIENTS

Balaadithya Uppalapati¹, Akash Kota², Vamsy P. Chodavarapu², Goutam Koley¹

¹Department of Electrical & Computer Engineering, Clemson University, Clemson, SC, USA

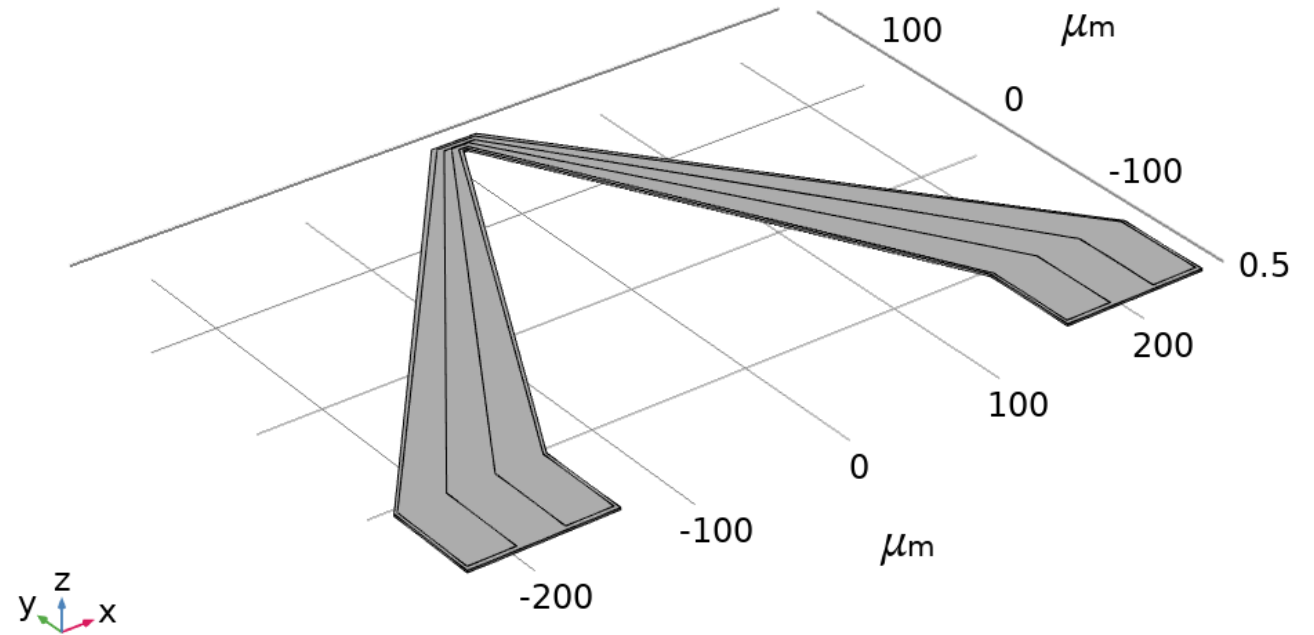
²Department of Electrical & Computer Engineering, University of Dayton, Dayton, OH, USA





Outline

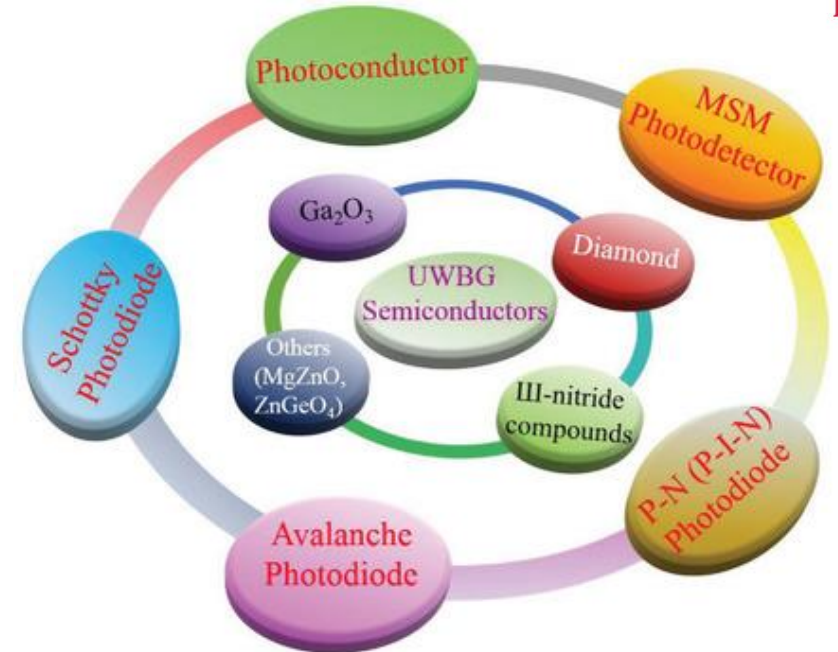
- Introduction
- Geometry Setup
- Simulation Procedure
- Results
- Summary





Introduction

- Cantilever has been modeled to compute the Fresnel coefficients like absorptance, reflectance, and transmittance in the wavelength range of 300 nm to 500 nm
- Fresnel coefficients are calculated for different thickness of bottom GaN layer
- Fresnel coefficients are also calculated by varying Al alloy composition in $Al_xGa_{(1-x)}N$



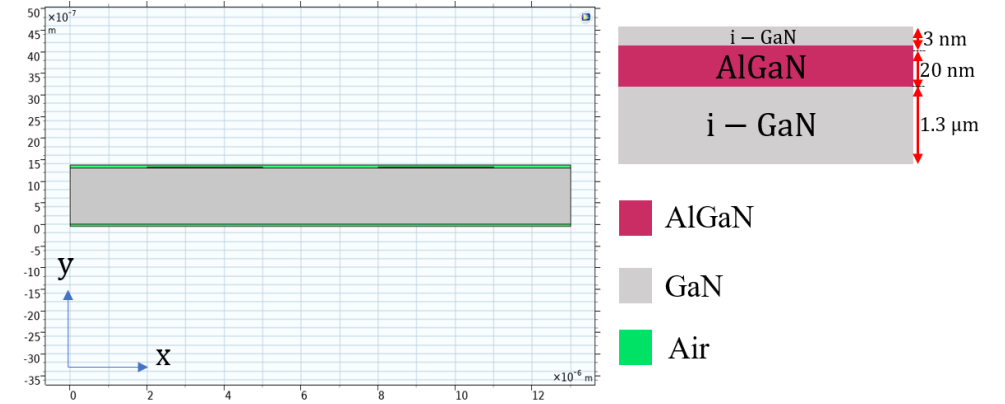
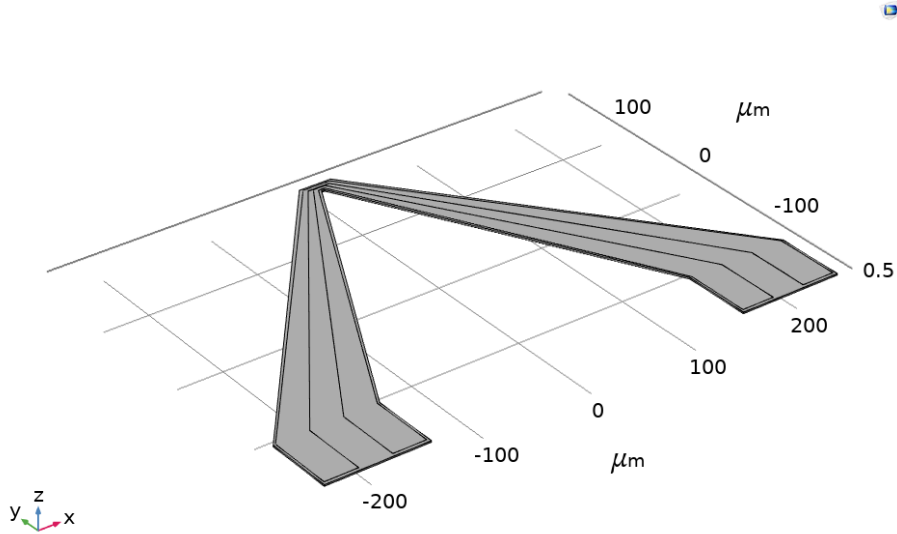
Source: C. Xie *et al.*, “Recent Progress in Solar-Blind Deep-Ultraviolet Photodetectors Based on Inorganic Ultrawide Bandgap Semiconductors,” *Adv. Funct. Mater.*, **29**, 1806006 (2019).

□ Applications

- Detect UV irradiation on Earth which can increase due to depletion of ozone layer
- Short wavelength UV light used for flame detection
- Solar blind cameras for monitoring electrical power lines
- Detection of high-temperature flames from rocket motor of a missile observed in intense sun light



Geometry Setup



3D Geometry of GaN–Al_xGa_{1-x}N–GaN ultraviolet photodetector

Longitudinal cross section at the tip region of the cantilever

- Simplified 2D geometry has been used in the finite element model
- Thicknesses of the top GaN, intermediate Al_xGa_{1-x}N, and bottom GaN layers are 3 nm, 20 nm, and 1 μm respectively
- The gap between the two adjacent Al_xGa_{1-x}N layers is 3 μm
- An air medium of 50 nm thickness is added throughout the width of the cantilever to consider the surrounding environment of the cantilever



Simulation procedure

- To get the electric field distribution on the 2D geometry, the governing equation to be solved can be written as

$$\nabla \times (\nabla \times E) - k_0^2 \epsilon_r E = 0, \quad (1)$$

where $k_0 = \frac{2\pi}{\lambda}$ is the free space propagation constant and ϵ_r is the relative permittivity of the material.

- For the given 2D geometry, the complex electric field E which is distributed along x and z axis can be written as

$$E(x, z) = \tilde{E}(x)e^{-jk_z z}, \quad (2)$$

where $\tilde{E}(x)$ represents the complex amplitude of the electric field distributed along the x axis and k_z is the out-of-plane wave vector component which is along the z direction.

- The relative permittivity of the material can be written as

$$\epsilon_r = (n - jk)^2, \quad (3)$$

where n and k are the respective real and imaginary parts of the refractive index of the material.

- In this simulation, the electrical conductivity (σ) and relative permeability (μ_r) of the material are assumed to be 0 and 1 respectively.



Simulation procedure cont....



University of
Dayton

- For the given 2D geometry the reflection (R) and transmission (T) coefficients are obtained by calculating the s -parameters.

- The reflection coefficient (R) is calculated as

$$R = |s_{11}|^2. \quad (4)$$

- The transmission coefficient (T) is calculated as

$$T = |s_{21}|^2. \quad (5)$$

- The equation to calculate s_{11} can be written as

$$s_{11} = \frac{\iint ((E_c - E_1) \cdot E_1^*) dA_1}{\iint E_1 \cdot E_1^* dA_1}, \quad (6)$$

where E_c is the computed electric field and E_1 is the electric field pattern on port 1.

- The computed electric field can be written as

$$E_c = \sum_{i=1} s_{i1} E_i. \quad (7)$$

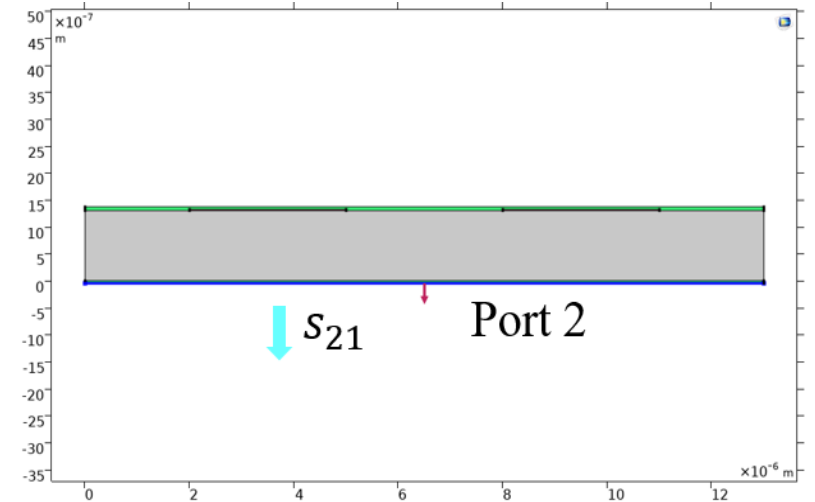
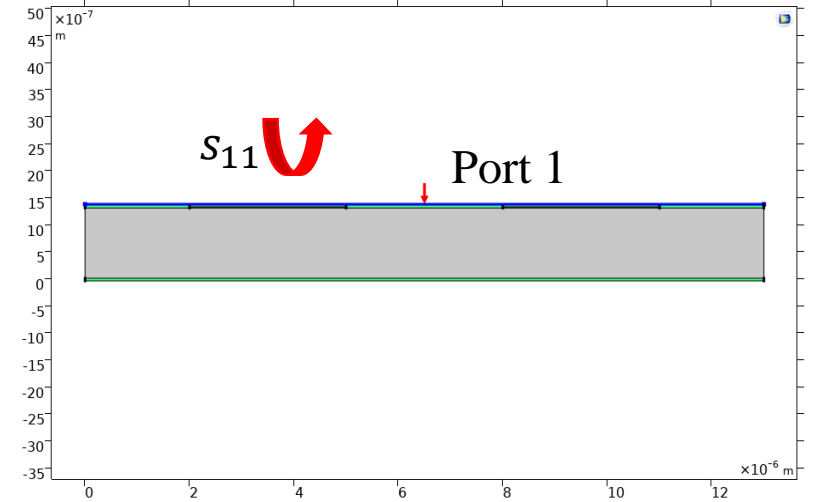
- The equation to calculate s_{21} can be written as

$$s_{21} = \frac{\iint (E_c \cdot E_2^*) dA_2}{\iint E_2 \cdot E_2^* dA_2}, \quad (8)$$

where E_2 is the electric field pattern on port 2.

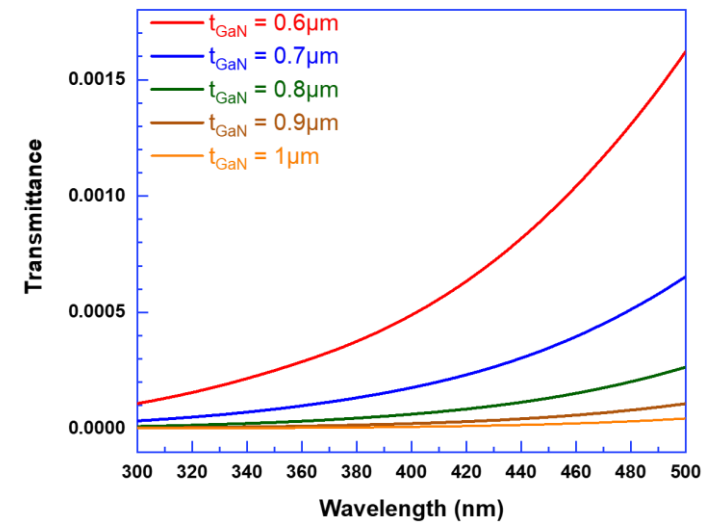
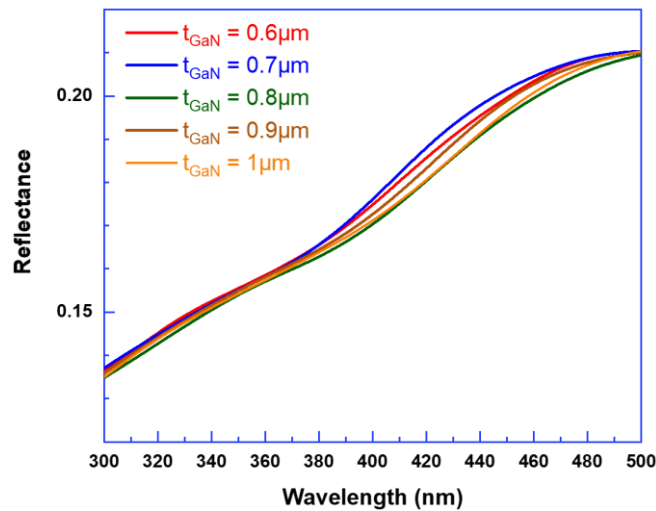
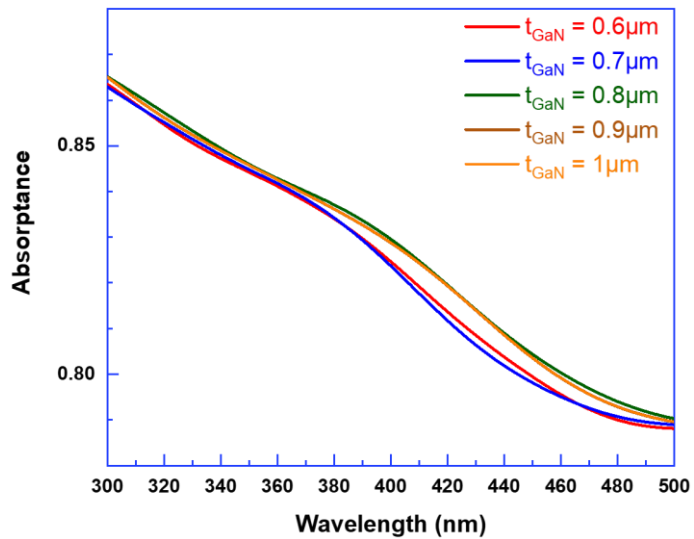
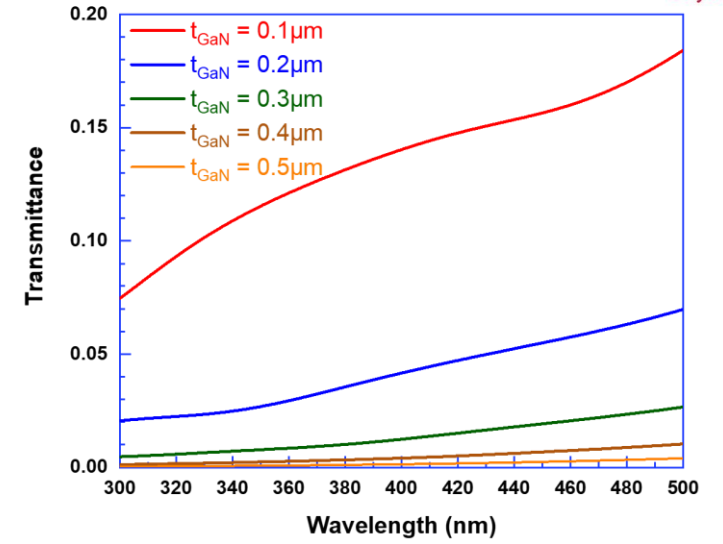
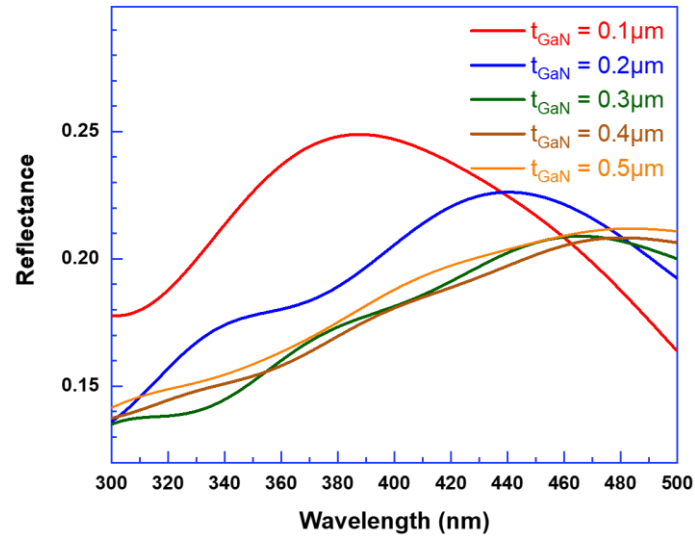
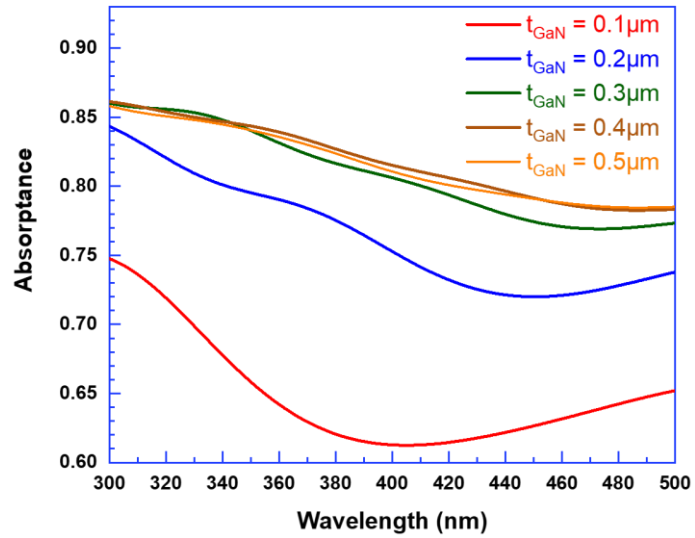
- The absorption coefficient (A) is calculated as

$$A = 1 - R - T \quad (9)$$



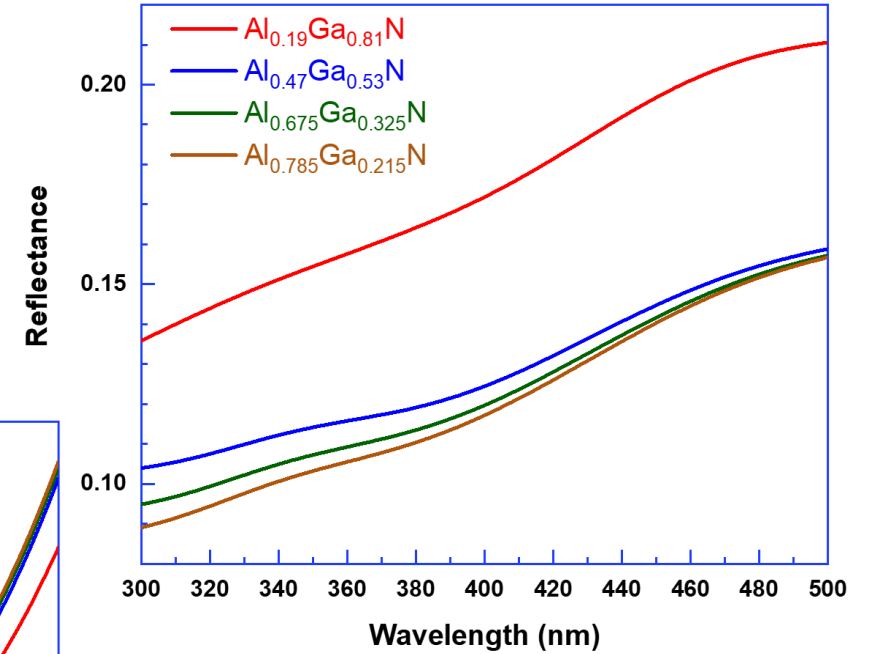
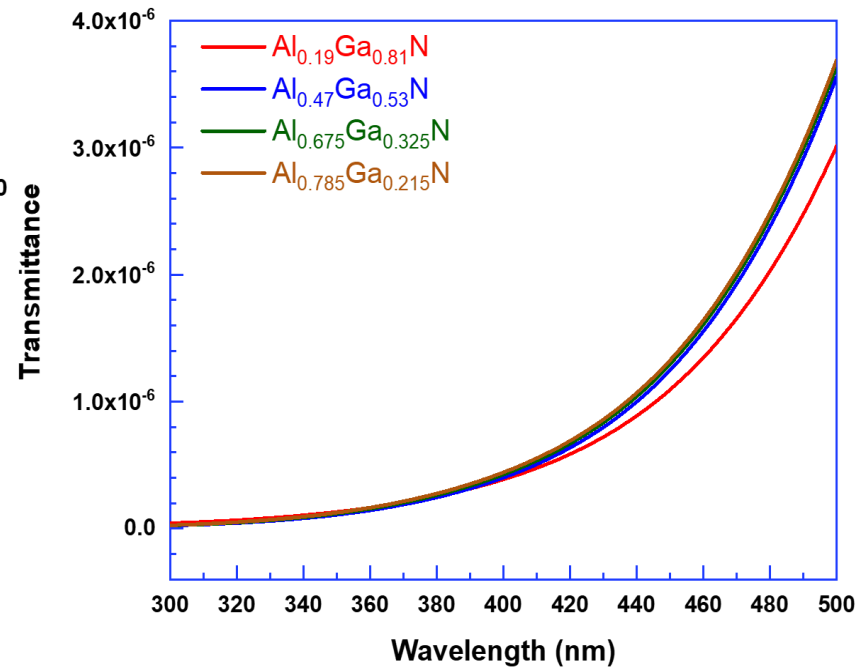
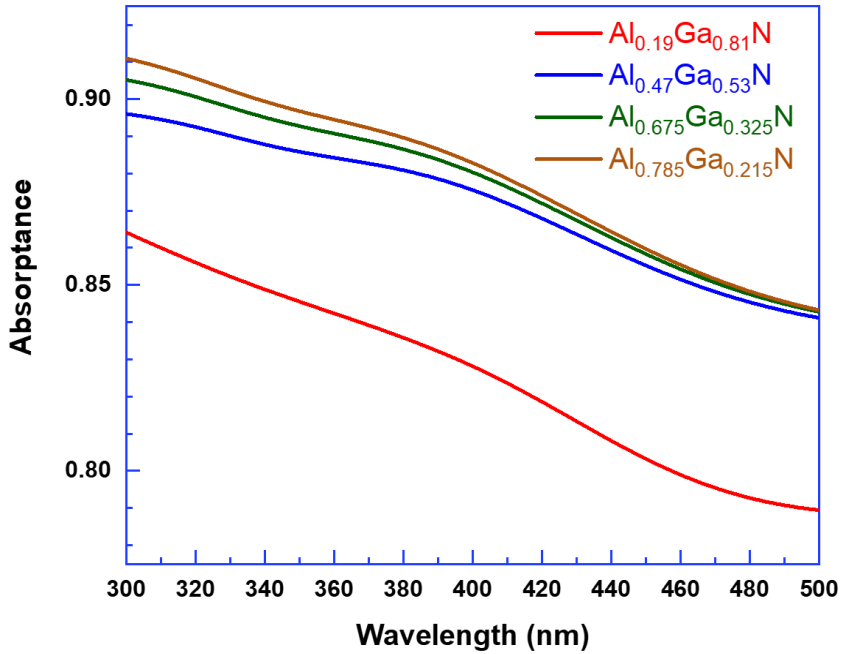


Fresnel coefficients for different thickness of GaN





Fresnel coefficients for different Al alloy composition in





Conclusion



- For bottom layer GaN thicknesses $> 0.5 \mu\text{m}$, the absorptance and reflectance profiles remains basically unchanged
- For thicknesses $< 0.5 \mu\text{m}$, the absorptance increases monotonically with the thickness of the bottom GaN layer
- From the simulations it has been observed that for thicknesses $\geq 1 \mu\text{m}$, the transmittance of UV light through the cantilever is zero
- With the thickness of the bottom GaN layer being fixed at $1.3 \mu\text{m}$, the effect of Al alloy composition in $\text{Al}_x\text{Ga}_{(1-x)}\text{N}$ on the Fresnel coefficients has also been studied
- From the simulation results, it can be concluded that at any given wavelength as the Al% increases, the absorptance and reflectance of the cantilever monotonically increases and decreases, respectively



References



1. A.Khan, K.Balalrishnan, and T.Katona, "Ultraviolet light-emitting diodes based on group three nitrides," *Nat. Photonics*, **2**, 77–84 (2008).
2. S. Zhao *et al.*, "An electrically injected AlGaIn nanowire laser operating in the ultraviolet-C band," *Appl. Phys. Lett.*, **107**, 043101 (2015).
3. A. Talukdar *et al.*, "Piezotransistive transduction of femtoscale displacement for photoacoustic spectroscopy," *Nat. Comm.*, **6**, 1-10 (2015).
4. D. Khan *et al.*, "Plasmonic amplification of photoacoustic waves detected using Piezotransistive GaN microcantilevers," *App. Phy. Letters.*, **111**, 062102 (2017).
5. F. Bayram *et al.*, "Piezotransistive GaN microcantilevers based surface work function measurements," *Jpn. J. Appl. Phys.*, **57**, 04030 (2018).
6. M. Razeghi and A. Rogalski, "Semiconductor ultraviolet detectors," *J. Appl. Phys.*, **79**, 7433-7473 (1996).
7. L. Sang, M. Liao, Y. Koide, M. Sumiya, "High-temperature ultraviolet detection based on InGaIn Schottky photodiodes," *Appl. Phys. Lett.*, **99**, 031115 (2011).
8. Y. Bie, Z. Liao, H. Zhang, G. Li, Y. Ye, Y. Zhou *et al.*, "Self-powered, ultrafast, visible-blind UV detection and optical logical operation based on ZnO/GaN nanoscale P-N junctions," *Adv. Mater.*, **23**, 649-653 (2011).
9. M. Khan *et al.*, "III–Nitride UV Devices," *Jpn. J. Appl. Phys.*, **44**, 7191–7206 (2005).
10. K. H. Lee *et al.*, "AlGaIn/GaN Schottky barrier UV photodetectors with a GaN sandwich layer," *IEEE Sens. J.*, **9**, 814–819 (2009).
11. T. Tut *et al.*, "Solar-blind Al_xGa_{1-x}N based avalanche photodiodes," *Appl. Phys. Lett.*, **87**, 223502 (2005).
12. H. Y. Liu, Y. H. Wang, and W. C. Hsu, "Suppression of dark current on AlGaIn/GaN metal-semiconductor-metal photodetectors," *IEEE Sens. J.*, **15**, 5202–5207 (2015).
13. E. Monroy, F. Calle, E. Munoz, and F. Omnes, "AlGaIn metal-semiconductor-metal photodiodes," *Appl. Phys. Lett.*, **74**, 3401–3403 (1999).
14. D. B. Li *et al.*, "Effect of asymmetric Schottky barrier on GaN-based metal-semiconductor-metal ultraviolet detector," *Appl. Phys. Lett.*, **99**, 261102 (2011).
15. X. J. Sun *et al.*, "High spectral response of self-driven GaN-based detectors by controlling the contact barrier height," *Sci. Rep.*, **5**, 16819 (2015).
16. E. Monroy *et al.*, "High-quality visible-blind AlGaIn p-i-n photodiodes," *Appl. Phys. Lett.*, **74**, 1171–1173 (1999).
17. D. Walker *et al.*, "Solar-blind AlGaIn photodiodes with very low cutoff wavelength," *Appl. Phys. Lett.*, **76**, 403–405 (2000).
18. R. McClintock *et al.*, "High quantum efficiency AlGaIn solar-blind pin photodiodes," *Appl. Phys. Lett.*, **84**, 1248–1250 (2004).
19. T. Tut, M. Gokkavas, A. Inal, and E. Ozbay, "Al_xGa_{1-x}N based avalanche photo-diodes with high reproducible avalanche gain," *Appl. Phys. Lett.*, **90**, 163506 (2007).
20. L. Sun, J. L. Chen, J. F. Li, and H. Jiang, "AlGaIn solar-blind avalanche photodiodes with high multiplication gain," *Appl. Phys. Lett.*, **97**, 191103 (2010).
21. Y. Huang *et al.*, "Back-illuminated separate absorption and multiplication AlGaIn solar-blind avalanche photodiodes," *Appl. Phys. Lett.*, **101**, 253516 (2012).
22. M. A. Khan *et al.*, "Schottky barrier photodetector based on Mg-doped p-type GaN films," *Appl. Phys. Lett.*, **63**, 2455 (1993).
23. H. Jiang *et al.*, "Visible-blind metal-semiconductor-metal photodetectors based on undoped AlGaIn/GaN high electron mobility transistor structure," *Jpn. J. Appl. Phys.*, **43**, L683 (2004).
24. E. Cicek *et al.*, "Al_xGa_{1-x}N based back-illuminated solar-blind photodetectors with external quantum efficiency of 89%," *Appl. Phys. Lett.*, **103**, 191108 (2013).
25. T. Kawashima, H. Yoshikawa, and S. Adachi, "Optical properties of hexagonal GaN," *J. Appl. Phys.*, **82**, 3528 (2003).
26. N. Antoine-Vincent, *et al.*, "Determination of the refractive indices of AlN, GaN, and Al_xGa_{1-x}N grown on (111) Si substrates," *J. Appl. Phys.*, **93**, 5222-5226 (2003).

